Doping in metal chalcogenide glasses

© S.A. Girlani, B. Yan, P.C. Taylor

University of Utah, Salt Lake City,
UT, USA

(Получена 16 марта 1998 г. Принята к печати 17 марта 1998 г.)

Chalcogenide glasses that contain sufficient concentrations of metal atoms can be doped *p*-type. This doping results in part because the local structural order is tetrahedral at both the metal and the chalcogen sites in these glasses. At concentrations exceeding 10^{19} см$^{-3}$, oxygen promotes doping by increasing the densities of dangling-bond defects at 3-fold-coordinated chalcogens, which are the doping sites in these glasses. For oxygen concentrations below 10^{19} см$^{-3}$, the conductivity is independent of oxygen and, therefore, is controlled by other mechanisms. The compositions $Cu_6As_4S_9$ and $Cu_6As_4Se_9$ are studied because at these compositions the S (or Se) and Cu atoms are all tetrahedrally coordinated and there exist only Cu–S and As–S (or Cu–Se and As–Se) bonds.

Introduction

These is strong experimental evidence [1–3] that many metal atoms, such as copper, are incorporated in chalcogenide glasses at tetrahedral sites. Based on the covalent nature of the local bonding, models of these glass structures [4–7] suggest that the chalcogen atoms also exist at tetrahedral sites when the metal concentrations are large enough. In ternary metal chalcogenide systems, such as Cu–As–S and Cu–As–Se, chemical ordering (Cu–S and As–S bonds only, for example) is preserved along a specific tie line in the ternary phase diagram. For the Cu–As–S and Cu–As–Se systems these tie lines are $(Cu_{2/3}S_{1/3})_x(As_{2/5}S_{3/5})_{1-x}$ and $(Cu_{2/3}S_{1/3})_x(As_{2/5}Se_{3/5})_{1-x}$ provided that $x \leq 9/19$. At $x = 9/19$ the stoichiometry is particularly simple: copper and chalcogen atoms are four-fold coordinated, arsenic atoms are three-fold coordinated, and there exist only Cu-chalcogen and As-chalcogen bonds. This composition, which can be expressed as $Cu_6As_4S_9$ or $Cu_6As_4Se_9$, corresponds to a well known crystalline structure, a natural mineral called sinnerite, where the numbers of nearest neighbors (local coordination numbers) are also 4, 3 and 4 for the copper, arsenic and sulfur atoms, respectively [8]. At even higher copper concentrations there are two well studied crystalline structures in the sulfur system that also occur as natural minerals, enargite [8], and luzonite [8]. Enargite exhibits the wurtzite structure and luzonite the zincblend structure. For all of these reasons, one may be reasonably confident that the nearest-neighbor order in the glasses $Cu_6As_4S_9$ and $Cu_6As_4Se_9$ is well understood.

Although the local structural order in the glasses, $Cu_6As_4S_9$ and $Cu_6As_4Se_9$, is reasonably well understood, much less is known about the electronic defects, especially those that contribute to large changes in *p*-type conductivity that have been observed [9–12]. In the prototypical chalcogenide glasses, such as As_2S_3 and As_2Se_3, the chalcogens are two-fold coordinated and the defects are dramatically influenced by strong electron-lattice interactions. In fact, these interactions are so strong that the characteristic defects possess negative effective electron-electron correlation energies (negative U^{eff}) that make the glasses impossible to dope. The two-fold coordination of the chalcogens results in non-bonding *p*-orbitals that form the highest-lying states in the valence band.

As far as the electronic states are concerned, the major difference between As_2S_3 or As_2Se_3 and $Cu_6As_4S_9$ or $Cu_6As_4Se_9$ is that the highest-lying states in the valence band in the latter compositions are made from sp^3 hybrids on the tetrahedrally coordinated Cu and chalcogen atoms. A second importrant distinction is that, because of the large increase in average, local coordination number, the flexibility of the lattice is drastically reduced for the compositions, $Cu_6As_4S_9$ or $Cu_6As_4Se_9$. In $Cu_6As_4S_9$ or $Cu_6As_4Se_9$ the average local coordination number is $n = 3.8$, which is similar to that of the hydrogenated amorphous silicon (*a*-Si : H) alloys used in thin-film transistors and solar cells. As a result, as in *a*-Si : H lattice relaxation plays little role for the characteristic defects in $Cu_6As_4S_9$ or $Cu_6As_4Se_9$ where the important defect identified with the doping site possesses a positive value for U^{eff} [9,13]. This defect has been attributed to an electron trapped at a dangling sulfur or selenium bond at a tetrahedral chalcogen site [9,10,13]. Presumably the wave function for this paramagnetic defect is predominantly sp^3 as is the case for the silicon dangling bond at a tetrahedral silicon site in *a*-Si : H.

Oxygen is a pervasive impurity in most chalcogenide glasses, and the glasses $Cu_6As_4S_9$ and $Cu_6As_4Se_9$ are no exception. As will be shown below addition of oxygen to these glasses increases the conductivities by more than three orders of magnitude [10,11]. The conductivity appears to be through extended stated and not simply a hopping conductivity in a defect band intoduced by the oxygen [10]. The doping sites have been ascribed [9] to the analog of cation vacancies that are known to produce *p*-type conductivity in $A^{II}B^{VI}$ crystals. One must be careful with this analogy since the concert of "missing Cu atoms at Cu sites" does not have the precise meaning that it does in crystalline solids. Since essentially all that is preserved in the amorphous solid is nearest-neighbor order, the signature of a "missing Cu at a Cu site" is the presence in the nominally stoichiometric glass of chalcogen–chalcogen bonds and chalcogen dangling bonds. These bonding configurations represent analogs in the glass to the reconstructed (Se–Se bonds) and unreconstructed (Se dangling bonds) nearest-neighbonrs of a Cu vacancy in the crystalline phase.

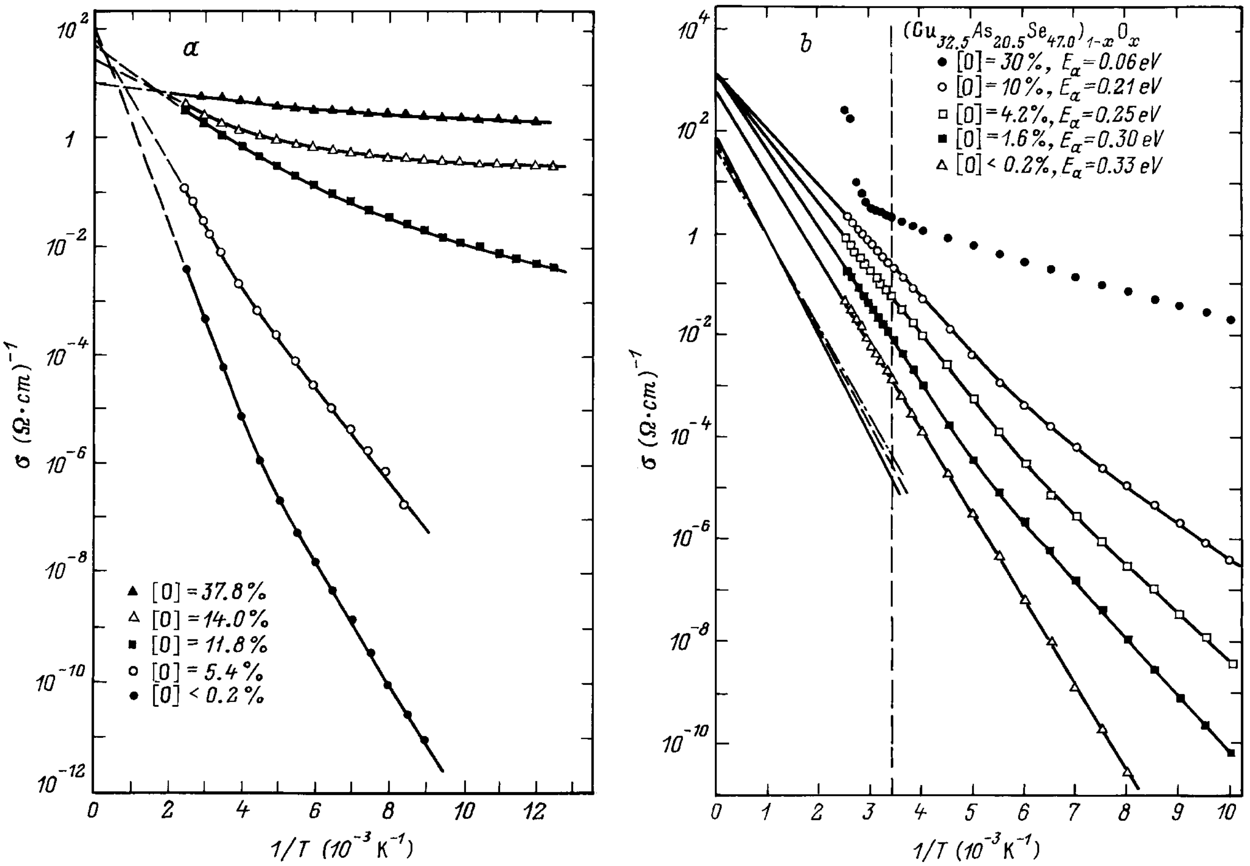

Figure 1. Electrical conductivity as a function of inverse temperature in a series of (*a*) $Cu_6As_4S_9$ glasses and (*b*) $Cu_6As_4Se_9$ glasses with varying oxygen concentrations [O]. Electrical activation energies can be determined from the higher temperature portions of the curves. The three lower curves (solid line, dashed line, dot-dashed line) in (*b*) represent conductivities for $(Cu_{2/3}Se_{1/3})_{0.14}(As_{2/5}Se_{3/5})_{0.86}$ glasses with 0.2, 10 and 30 at% oxygen, respectively.

It is kind of reasoning that leads to the attribution of the doping site in $Cu_6As_4S_9$ or $Cu_6As_4Se_9$ glasses to chalcogen dangling bonds at tetrahedral chalcogen sites. Electron spin resonamce (ESR) measurements [9,10,13] on both $Cu_6As_4S_9$ and $Cu_6As_4Se_9$ are consistent with this interpretation. The ESR spectra are attributed to paramagnetic spins located on chalcogen atoms, and the lineshapes are different from those attributed to spins on chalcogen atoms at sites that are normally two-fold coordinated, such as those that occur in As_2S_3 and As_2Se_3.

The energy levels in the gap for the chalcogen, dangling-bond defects that generate the doping are not well known, but optical absorption measurements [9,12] show an absorption below the optical gap that scales with the electrical conductivity. This absorption rises at about 0.4 eV in $Cu_6As_4S_9$ [12] and at about 0.2 eV in $Cu_6As_4Se_9$ [9].

It this paper we review the measurements of electrical conductivity, optical absorption and ESR in oxygen-doped and nominally undoped $Cu_6As_4S_9$ and $Cu_6As_4Se_9$ glasses. We discuss the evidence for the *p*-type conduction process, and we present a microscopic picture for the defects that produce the doping effect.

Experimental details

Because the glass-forming regions in the Cu–As–S and Cu–As–Se systems do not include the $Cu_6As_4S_9$ and $Cu_6As_4Se_9$ compositions, all samples studied were prepared by sputtering. Normally, the films were deposited on glass or ESR-grade quartz substrates. Sputtering targets were made from ceramic samples of the appropriate composition. Bulk samples were powdered and pressed at 6000 psi and 200°C. Ultra-high purity argon was used as the sputtering gas, and oxygen was introduced to produce intentionally-doped samples. Details of the sputtering procedures are available elsewhere [11,14]. Typical sample thicknesses were 1 to 5 μm. Glass compositions were measured using electron microprobe analysis, and impurity concentrations using secondary ion mass spectroscopy (SIMS). Electrical measurements were performed using evaporated gold contacts. Variable temperatures were obtained using standard He-flow cryostats. Optical absorption experiments employed standard infrared and visible spectrometers. ESR measurements were made using a 9 GHz spectrometer (Bruker ER200D-SRC) and standard techniques to obtain variable temperatures. Details of the measurement apparatus and techniques are available elsewhere [14].

Results

The variations of the electrical conductivities in $Cu_6As_4S_9$ and $Cu_6As_4Se_9$ glasses with oxygen concentration are shown in Figs. 1, *a* and 1, *b*, respectively. From this figure it is clear that oxygen dramatically changes the temperature dependence of the electrical conductivity and hence the activation energies extracted from the data. The trends are obvious. The conductivity at a given temperature increases dramatically with oxygen concentration and the activation energy decraeses correspondingly. (The rapid rise in conductivity at high temperatures for the sample of glassy $Cu_6As_4Se_9$ with 30 at% oxygen is due to crystallization of the sample.) Although the breaks in the slopes at low temperatures may be evidence for hopping conductivity, the values of the prefactors for the thermally-activated conductivities at higher temperatures are consistent with conduction involving extended states.

Figure 1, *b* also shows data for a sample of Cu–As–Se where the copper concentration is 21 at%, which is lower than in $Cu_6As_4Se_9$ (where the Cu concentration is nominally 31.5 at%). For this lower copper concentration, shown by the lines without data points in Fig. 1, *b*, simple bonding models, such as the formal valence shell or FVS model [5,7], suggest that the copper and arsenic remain four- and three-fold coordinated, respectively, but that the chalcogen is essentially three-fold coordinated. (The average local coordination number for selenium at this composition is calculated to be 3.2.) It is clear from Fig. 1, *b* that for the glass where the chalcogen is mostly three-fold coordinated, there is little if any doping generated by the presence of oxygen. One therefore requires tetrahedral coordination of the chalcogen for the *p*-type doping process to occur.

For oxygen concentrations above about $3 \times 10^{19}\,cm^{-3}$, the dark conductivity at a given temperature scales linearly with the oxygen content. This behavior is shown for $Cu_6As_4S_9$ glasses in Fig. 2. For oxygen concentrations below $3 \times 10^{19}\,cm^{-3}$, the conductivity becomes insensitive to oxygen content. Therefore, below this critical value of oxygen concentration another mechanism determines the number of defects that control the doping in the glass. It is probable that at these low oxygen levels the defect formation is determined by kinetics during growth as is often the case for the densities of vacancies and intersitials during the growth of $A^{II}B^{VI}$ crystals.

A second example of the lack of correlation between oxygen concentration and electrical conductivity for low oxygen concentrations is shown in Fig. 3. In this figure the conductivities are plotted as a function of the measured activation energies. The data in Fig. 3 follow the usual trend that the activation energy scales inversely with the log of the electrical conductivity at a given temparature. A comparison with Fig. 2 shows that the oxygen concentrations differ by an order of magnitude for the two glasses with activation energies between 0.38 and 0.40 eV.

There exists an optical absorption band that scales with the electrical conductivity and with the oxygen concentration for high oxygen content ($> 3 \times 10^{19}\,cm^{-3}$). This absorption is shown for $Cu_6As_4S_9$ glass in Fig. 4. A similar plot exists for $Cu_6As_4Se_9$ glass [9,12] except that the absorption for the selenium glasses rises near 0.2 eV while for the sulfur glasses shown in Fig. 4 the absorption rises near 0.4 eV. For oxygen concentrations below $3 \times 10^{19}\,cm^{-3}$, the absorption cannot be distinguished from the exponential band-gap absorption that is always present. The fact that this absorption scales with the electrical conductivity suggests that the onsets (0.2 and 0.4 eV in the selenium and sulfur glasses, respectively) can be associated with the energies of the acceptor levels with respect to the valence band mobility edge.

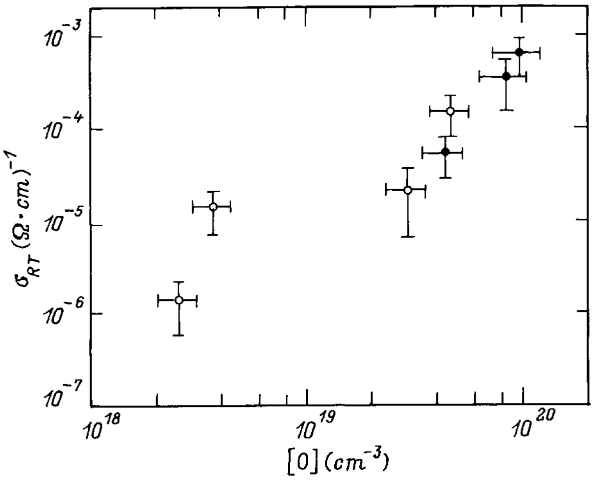

Figure 2. Electrical conductivity at 300 K (σ_{RT}) as a function of oxygen concentration ([O]) in $Cu_6As_4S_9$ glasses. Closed and open circles represent intentionally oxygen-doped and nominally undoped films, respectively.

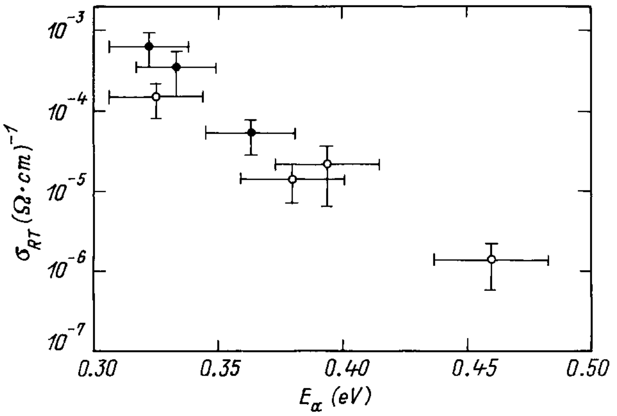

Figure 3. Electrical conductivity at 300 K (σ_{RT}) as a function of activation energy for conduction (E_a) for various films of glassy $Cu_6As_4S_9$. Closed and open circles represent intentionally oxygen-doped and nominally undoped films, respectively.

The microscopic nature of these doping sites can be elucidated by measuring the ESR spectra of $Cu_6As_4S_9$ and $Cu_6As_4Se_9$ glasses with varying electrical conductivities. As mentioned above, the lineshapes of the ESR spectra indicate

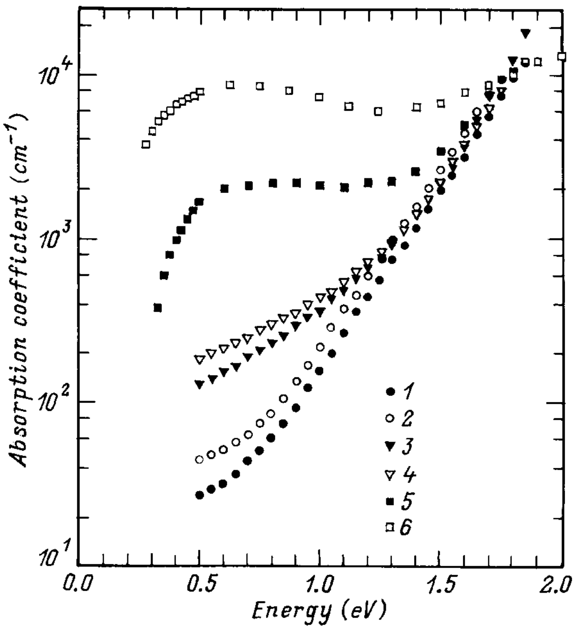

Figure 4. Optical absorption coefficient as a function of energy for glassy $Cu_6As_4S_9$ films. Oxygen concentrations [O], $10^{19}\,cm^{-3}$: *1* — 3.0, *2* — 4.4, *3* — 8.5, *4* — 9.8, *5* — 18, *6* — 45.

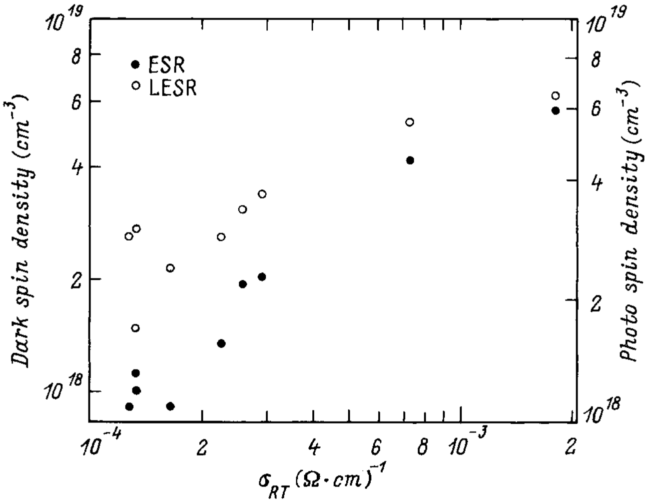

Figure 5. ESR spin densities at 20 K as a function of electrical conductivity at 300 K σ_{RT}) in various films of glassy $Cu_6As_4S_9$. Filled and open circles represent dark and metastable, photo-induced spin densities, respectively.

that the electronic states are closely associated with the chalcogen atoms. In particular, these lineshapes have been attributed [9,10,13] to holes trapped at sulfur or selenium "dangling bonds" where the site symmetries remain essentially tetrahedral. If this is the case, then the unpaired spin resides predominantly in an sp^3 hybrid orbital on the chalcogen atom much as is the case for the silicon dangling bond in *a*-Si and *a*-Si : H. Figure 5 shows the intensity of this ESR signal in $Cu_6As_4S_9$ glass as a function of the electrical conductivity. For technical reasons, the ESR is measured at low temperatures (20 K) while the conductivity is measured at room temperature (~ 300 K), but this detail should not affect the proportionality between the two measurements provided that the electronic levels contributing to the *p*-type conductivity are the paramagnetic centers measured by ESR. From the data of Fig. 5 (filled circles) it appears that this assumption is correct. It is interesting to note that although the conductivity does not scale with oxygen concentration at low oxygen concentrations, the conductivity does scale with the ESR for all oxygen levels. This result means that although oxygen does not determine the densities of defects when the oxygen concentrations are low, the defects that are formed and measured by ESR do control the conductivity. Because the ESR lineshape does not change, the same defects (holes trapped at 3-fold-coordinated chalcogen sites) determine the conductivities in all samples.

Also plotted in Fig. 5 are metastable, photo-induced increases in the ESR spin densities, similar the photo-induced ESR observed in glassy As_2S_3 and As_2Se_3 at low temperatures. However, in this case the photo-induced ESR results in a concomitant increase in the dark conductivity (so-called persistent photoconductivity) at low temperatures [13], as would be expected since these sites contribute to the electrical conductivity in the $Cu_6As_4S_9$ and $Cu_6As_4Se_9$ glasses. The mechanism for optically activating these additional acceptor sites is not known at present.

Discussion

From the data presented in the previous section, a consistent model emerges to explain the electrical conductivity in the tetrahedrally coordinated chalcogenide glasses. When metals, such as the Group I metal — copper, are added to chalcogenide glasses, the average local coordination number of the chalcogen increases to four from its usual value of two. Concomitant with this increase in average local coordination number is a change in the characteristic defects that are formed. In place of the "soft" lattice in As_2S_3 or As_2Se_3 is a "hard" lattice in $Cu_6As_4S_9$ or $Cu_6As_4Se_9$. This change means that the characteristic defects possess a positive effective electron-electron correlation energy, and if the defect energies are close enough to the valence or conduction band edges, then doping can occur.

In glassy $Cu_6As_4S_9$ or $Cu_6As_4Se_9$ the characteristic defect is found to be a hole trapped at a tetrahedral chalcogen site due to the fact that one of the four nearest-neighbor bonds is missing. The production of these defects can be enhanced by the incorporation of oxygen in the glasses, but there appears to be a basic, lower level for these defects that is controlled by the kinetics during growth.

An analogy between the doping in $A^{II}B^{VI}$ crystals by vacancies and interstitials and the doping in $Cu_6As_4S_9$ and $Cu_6As_4Se_9$ glasses is useful. This analogy makes some sense because in both the crystals and the glasses the structure is strongly influenced by the covalent nature of the bonds, but the defects are dominated by ionic considerations. In $A^{II}B^{VI}$ crystals one type of vacancy or vacancy-interstitial pair tends to dominate in a specific crystal. Therefore, a $A^{II}B^{VI}$ crystal tends to be either *p*-type or *n*-type, and it is very difficult to change the carrier type. This trend occurs because one type of vacancy (cation or anion) dominates in any given crystal and because cation vacancies generate *p*-type conduction while anion vacancies generate *n*-type conduction.

To the extent that this analogy holds, one would expect that *n*-type conductivity would be very difficult to achieve in glassy $Cu_6As_4S_9$ or $Cu_6As_4Se_9$. To date, this expectation has been fulfilled since attempts to co-dope with other elements or to compensate for the chalcogen-based acceptors have all failed. Assuming that substitutional doping is as difficult to achieve in the tetrahedrally-coordinated chalcogenide glasses as it is in the $A^{II}B^{VI}$ crystals, one might expect that the only hope to produce *n*-type conductivity is to change the host lattice. Again by analogy with the $A^{II}B^{VI}$ crystals, the production of anion vacancies is promoted by decreasing the size of the anion with respect to the cation. To date, attempts to do the same in the tetrahedrally-coordinated chalcogenide glasses have also failed perhaps because the larger cations (metals) tend to form fewer than four bonds in the glasses.

Summary

As metals are added to the chalcogenide glasses the average, local coordination number of the chalcogen atoms increases from two to four. When the chalcogens are tetrahedrally coordinated, the glasses can be doped *p*-type. The addition of oxygen to the glass generates an increase in the *p*-type conductivity, but at low oxygen concentrations ($< 10^{19}\,\mathrm{cm}^{-3}$) residual doping sites exist that are probably determined by the kinetics during growth. From optical absorption measurements the doping levels for the acceptors are determined to be approximately 0.4 and 0.2 eV from the valence band mobility edge in glassy $Cu_6As_4S_9$ and $Cu_6As_4Se_9$, respectively. From ESR measurements the doping site is determined to be a hole trapped at a three-fold coordinated chalcogen site which retains its tetrahefral symmetry. That is, the hole exists predominantly in an sp^3-hybridized orbital on the chalcogen atom as opposed to the *p* orbital for the hole generated in the prototypical chalcogenide glasses, such as As_2S_3 and As_2Se_3. As expected, the doping sites in glassy $Cu_6As_4S_9$ and $Cu_6As_4Se_9$ possess positive, effective, electron-electron correlation energies.

Acknowledgments

This research was supported by the National Science Foundation under grant No. DMR-9704946. This work greatly benefitted from previous collaborations with J. Hautala, J.Z. Liu, B. Moosman, Z.M. Saleh and R.E. Shirey. The authors express their sincere appreciation for the seminal contributions of Professor B.T. Kolomiets to research on the chalcogenide glasses. His efforts inspired much of the subsequent research in this field.

References

[1] K.S. Liang, A. Bienenstock, C.W. Bates. Phys. Rev. B, **10**, 1528 (1974).
[2] S. Laderman, A. Bienenstock, K.S. Liang. Sol. Energy Mater., **8**, 15 (1982).
[3] S.H. Hunter, A. Bienenstock, T.M. Hayes. In: *Amorphous an Liquid Semiconductors*, ed. by W.E. Spear (University of Edinburgh, Edingurgh, 1977) p. 78.
[4] J.Z. Liu, P.C. Taylor. Phys. Rev. Lett., **59**, 1938 (1987).
[5] J.Z. Liu, P.C. Taylor. Sol. St. Commun., **70**, 81 (1989).
[6] J.Z. Liu, P.C. Taylor. J. Non-Cryst. Sol., **114**, 25 (1989).
[7] P.C. Taylor., Z.M. Saleh, J.Z. Liu. In: *Advances in Dicordered Semiconductors*, ed. by H. Fritzsche (World Scientific, Singapore, 1990) v. 3, p. 23.
[8] A.S. Wells. *Structural Inorganic Chemistry* (Clarendon, Oxford, 1975).
[9] J. Hautala, P.C. Taylor. In: *Optical Processes in Dicordered Solids*, ed. by Z.V. Vardeny ang P.C. Taylor (Elsevier, Amsterdam, 1991).
[10] J. Hautala, B. Moosman, P.C. Taylor. J. Non-Cryst. Sol., **137&138**, 1043 (1991).
[11] R.E. Shirey, P.C. Taylor. Univ. Utah. J. Undergrad. Res., **3**, 40 (1992).
[12] P.C. Taylor, R.E. Shirey, S. Girlani, J. Hautal. J. Non-Cryst. Sol., **164–166**, 1191 (1993).
[13] B. Yan, S. Girlani, P.C. Taylor. Phys. Rev. B, **56**, 1 (1997).
[14] S.A. Girlani. Ph. D. Thesis (1998).

Редактор Т.А. Полянская